RESEARCH ARTICLE

Claus Bundesen · Axel Larsen · Søren Kyllingsbæk ·
Olaf B. Paulson · Ian Law

Attentional effects in the visual pathways: a whole-brain PET study

Abstract Attentional effects in the visual pathways were investigated by contrasting the distribution of regional cerebral blood flow (rCBF) measured by $H_2^{15}O$ positron emission tomography (PET) during performance of a shape-matching task with the distribution of rCBF during a less demanding color-matching task. The two tasks were performed using the same stimuli: pairs of colored random shapes shown at a fixed rate (2 s per pair). In the shape-matching task, the subjects determined whether the two stimuli were the same in shape regardless of differences in size or color. In the color-matching task, the subjects determined whether the two stimuli were the same in color regardless of differences in size or shape. Mean reaction time for shape-matching exceeded mean reaction time for color-matching by nearly 200 ms. The corresponding shape-color comparison showed extensive bilateral increases in rCBF in visual areas in the occipital and parietal lobes, including the primary visual cortex. Subcortical activations were found in cerebellum (particularly the vermis) and in the thalamus with the focus in a region comprising the lateral geniculate nucleus, the pulvinar, and adjacent parts of the reticular nucleus. Frontal activations were found in a region that seems implicated in visual short-term memory (posterior parts of the superior sulcus and the middle gyrus). The reverse, color-shape comparison showed bilateral increases in rCBF in the anterior cingulate gyri, superior frontal gyri, and superior and middle temporal gyri. The attentional effects found by the shape-color comparison in the thalamus and the primary visual cortex may have been generated by feedback signals preserving visual representations of selected stimuli in short-term memory.

Keywords Working memory · Thalamus · Striate · Exstrastriate · Parietal · Prefrontal

C. Bundesen (✉) · A. Larsen · S. Kyllingsbæk
Department of Psychology, University of Copenhagen,
Njalsgade 90, 2300 Copenhagen S, Denmark
e-mail: claus.bundesen@psy.ku.dk
Tel.: +45-3532 8811
Fax: +45-3532 8745

O.B. Paulson · I. Law
Neurobiology Research Unit, N9201, and PET and Cyclotron Unit,
KF 3982, The Copenhagen University Hospital, Rigshospitalet,
Denmark

Introduction

This article presents a positron emission tomography (PET) study of attentional effects in the visual system. The study showed widespread attentional effects (effects of the experimental task when stimulus conditions were kept constant) ranging from the thalamus and area V1 [the primary (striate) visual cortex] up to prefrontal cortical regions that seem involved in visual short-term memory (VSTM). We conjecture that the attentional effects in the thalamus and area V1 were generated top-down by feedback signals serving to maintain representations of selected stimuli in VSTM ("working memory"), and we show that the same conjecture can explain many findings from related studies.

Several studies of brain activation using functional magnetic resonance imaging (fMRI) have shown effects of visual-spatial attention in early visual areas, including area V1 (Brefczynski and DeYoe 1999; Martínez et al. 1999; see also Shulman et al. 1997). For example, in the study by Martínez et al. (1999), subjects discriminated patterned targets presented among distractors, and blood oxygenation level-dependent (BOLD) contrast fMRI images indicated increase in regional cerebral blood flow (rCBF) and, hence, stronger neural activity in area V1 when the subject attended to the visual hemifield (left versus right) in which the stimulus display appeared than when the subject attended to the opposite hemifield. However, recordings of event-related potentials (ERPs) and modeling of their neural sources indicated that the initial sensory response of V1 to the stimulus display was unaffected by attention. Thus, modeling of the voltage topography of the earliest ERP component (the C1 component, with an onset latency of 50–60 ms) pointed

to a neural generator in V1, and this component showed no effects of attention. Previous ERP studies also failed to find evidence of attentional effects in V1 (cf. Clark and Hillyard 1996; Hillyard et al. 1997, 1998; Mangun et al. 1997; Woldorff et al. 1997; see also Clark et al.1995). To resolve the discrepancy between the fMRI data and the ERP data, Martínez et al. (1999) hypothesized that the attentional modulation found in V1 with fMRI represented (1) a sustained top-down activation of neurons in V1 during spatial attention, or (2) a delayed, re-entrant feedback from higher visual areas. The hypothesis raises questions concerning the existence and the possible function of the (sustained or delayed) top-down activation.

There is evidence against the notion of sustained top-down activation of neurons in V1 during spatial attention. Luck et al. (1997) found clear evidence of sustained top-down activation of neurons in monkey visual cortex during spatial attention, but the effect was limited to extrastriate areas. Specifically, by single-cell recordings in areas V2 and V4, spontaneous firing rates were 30–40% higher when attention was directed inside rather than outside the receptive field, even when no stimulus was present in the receptive field. In contrast, there was no increase in the baseline firing rate in area V1 when attention was directed inside the receptive field.

In a related fMRI study, Kastner and colleagues instructed subjects to covertly direct attention to a particular location and "to expect the occurrence of the stimulus presentations" at the given location so that they were ready to count the number of occurrences of a prespecified target pattern (see p 752 in Kastner et al. 1999). Whereas Luck et al. (1997) consistently used the same stimulus (a square) as the target, the stimulus to be expected in the study of Kastner et al. (1999) varied from trial to trial. With this design, Kastner et al. (1999) found increased activity in striate cortex, exstrastriate visual cortex, and frontal and parietal areas during the expectation period (i.e., in the absence of visual stimulation). It seems likely that during the expectation period, subjects maintained a mental image of the stimulus to be expected in VSTM. Maintaining the image in VSTM may have generated the activity found both in the visual cortex and in frontal and parietal areas.

A plausible function of delayed, re-entrant feedback from higher visual areas to early areas such as V1 is suggested by theories of visual attention in which attentional selection implies encoding into VSTM. For example, in the computational theory of visual attention called TVA (Bundesen 1990, 1998; Duncan et al. 1999; Logan 1996), perceptual categorization of a visual stimulus implies attentional selection of the stimulus, and the attentional selection is done by encoding the stimulus into VSTM. In a neural network implementation of TVA (Bundesen 1991, 2002), a stimulus is encoded into VSTM by activating a unit that represents the stimulus in a VSTM "map of locations". When this unit is activated, bottom-up signals that arrive at the unit from representations of the stimulus in lower visual areas are projected back whence they came. Thus, when a stimulus is represented in the VSTM map of locations, representations of the stimulus in lower visual areas are kept active by re-entrant feedback from the VSTM map. Anatomically the VSTM map may be found in prefrontal cortex, where regions implicated in visual short-term memory have been tentatively identified by fMRI in posterior parts of the superior frontal sulcus and the middle and inferior frontal gyri (Courtney et al. 1998; see also Smith and Jonides 1997).

In the study of Martínez et al. (1999), stimulus presentations were brief, so encoding of selected stimuli into VSTM could serve an obvious function by enabling continued analysis of targets after stimulus offset. However, if attentional selection consists in encoding into short-term memory (working memory), encoding of selected visual stimuli into VSTM should occur whether or not analysis of the stimuli must be continued after stimulus offset. Thus, if the attentional effects observed in V1 represent encoding into VSTM (a visual working memory), similar effects should appear in behavioral paradigms in which response selection occurs before stimulus offset.

In this article we report a PET study of attentional effects in the visual system. We compared the distribution of rCBF during performance of a time-consuming shape-matching task with that during a much less time-consuming color-matching task. The two tasks were performed using exactly the same stimuli (pairs of colored random shapes), and the stimuli were shown at a relatively slow rate (2 s per pair, including a blank interstimulus interval of 860 ms) so that selection of responses occurred before stimulus offset. In the shape-matching task, the subjects should determine whether the two stimuli were the same in shape regardless of differences in size or color. In the color-matching task, the subjects should determine whether the two stimuli were the same in color regardless of differences in size or shape. We expected that stimuli would be encoded into visual working memory (VSTM) in either task, but the stimuli should be retained in VSTM for a longer period of time in the shape-matching than in the color-matching task. The complete brain volume was PET scanned, and we looked for attentional effects (effects of the experimental task) both early and late in the visual system. We were particularly interested in effects in the primary visual cortex, possible effects at still lower, subcortical levels of processing, and effects in prefrontal cortical regions that are implicated in visual short-term memory.

Materials and methods

Subjects
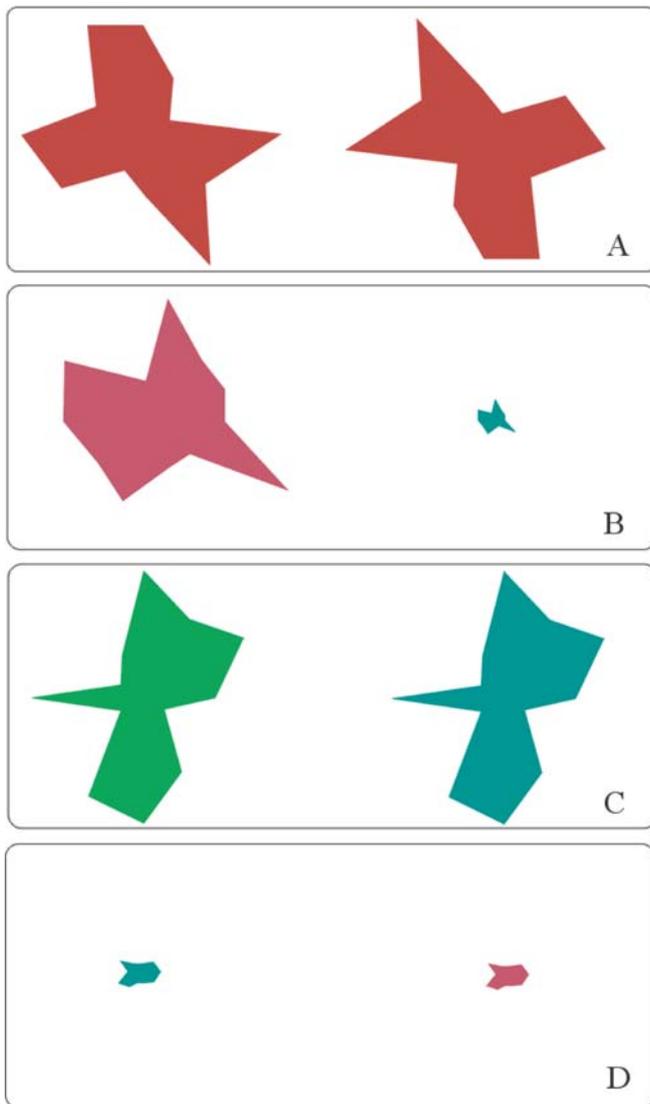
Fig. 1A–D Examples of stimulus pairs. **A** Different-shaped, same-colored (*rr*) stimulus pair with a size ratio of 1. **B** Same-shaped, different-colored (*r'g'*) stimulus pair with a size ratio of 6. **C** Same-shaped, different-colored (*gg'*) stimulus pair with a size ratio of 1. **D** Same-shaped, different-colored (*g'r'*) stimulus pair with a size ratio of 1

and the study was approved by the local ethics committee of Copenhagen [J. Nr. (KF) 01-339/94].

Stimuli

The stimulus patterns were colored random polygons (see Fig. 1) shown on the black face of a computer-driven cathode ray tube (CRT). To generate a polygon, 12 random numbers were drawn from a uniform distribution between 0.1 and 1. The numbers were taken to be the lengths of 12 evenly spaced, imaginary half-lines originating at the center of a unit circle. The direction of the first half-line ($v°$) was determined at random, and the polygon was constructed by connecting the endpoint of the first half-line with the endpoint of the second (i.e., the half-line with direction $v° + 30°$), the endpoint of the second half-line with the endpoint of the third ($v° + 60°$),..., and the endpoint of the 12th half-line ($v° + 330°$)

Table 1 Stimulus conditions 1–4

Size ratio	Color discriminability	
	High	Low
1	1	2
6	3	4

with the endpoint of the first, all connections being made by straight lines.

A stimulus pattern could be shown in a small format (size format 1) or in a large format (size format 6). Small patterns were generated by mapping the unit circle to a circle with a radius of 27 pixels (approximately 0.7°) on the CRT. Large patterns were generated by mapping the unit circle to a circle with a radius of 162 pixels (4.1°). The patterns appeared as solid shapes on a black (0 cd/m^2) background. Each pattern was colored in one of two highly similar shades of red (CIE *xy* coordinates of 0.27/0.60 at 20.8 cd/m^2, and 0.25/0.54 at 21.1 cd/m^2, respectively) or one of two highly similar shades of green (CIE *xy* coordinates of 0.58/0.31 at 13.9 cd/m^2, and 0.61/0.34 at 13.6 cd/m^2, respectively).

Each stimulus display consisted of two patterns (colored polygons) side by side. The polygons were centered symmetrically around a small fixation mark in the middle of the screen. The center-to-center distance between the polygons was 8° of visual angle at the viewing distance of 80 cm. Each pair of polygons was exposed for 1,142 ms. Consecutive pairs were separated by a blank interstimulus interval of approximately 860 ms.

Tasks

Two reaction-time tasks were investigated: shape-matching and color-matching. In shape-matching, the subjects' task was to indicate as quickly as possible whether the two patterns in the stimulus display were of the same shape. The subjects were informed that the two patterns should be considered to be the same in shape if, and only if, they were identical up to a translational displacement in the picture plane, a change in size, and a change in color. In color-matching, the task was to indicate as quickly as possible whether the two patterns in the stimulus display were of the same color. In both tasks, positive ("same") responses were indicated by pressing a right-hand mouse button, and negative ("different") responses were indicated by pressing a left-hand mouse button.

Stimulus conditions

Each of the two tasks were investigated in four different stimulus conditions (see Table 1). In every condition, some stimulus pairs were both same-shaped and same-colored (probability 0.25); some were same-shaped but not same-colored (probability 0.25); some were same-colored but not same-shaped (probability 0.25); and some were neither same-shaped nor same-colored (probability 0.25). To make the shape-matching task more difficult, members of a pair that were different in shape differed by just a rotation of 180° in the picture plane, in addition to possible differences in size and color (cf. Experiment 2 in Bundesen and Larsen 1975; Experiment 1 in Larsen and Bundesen 1978).

In stimulus condition 1, members of a stimulus pair were identical in size (size ratio 1), so shape-matching should be relatively easy. For members that differed in color, the colors (red versus green) were highly discriminable, so color matching should also be relatively easy. The 16 combinations of size formats and colors that were used in stimulus condition 1 are listed in Table 2. During a PET scan in which a given stimulus condition was used, the subject was presented with three consecutive blocks of 32 randomly ordered stimulus pairs; each of the three blocks contained

Table 2 Combinations of size formats and colors in stimulus condition 1. The characteristics of the two patterns (*Left* and *Right*) of each stimulus are shown (*r* and *r'* are two similar shades of red; *g* and *g'* are two similar shades of green)

Combination	Size format		Color	
	Left	Right	Left	Right
1	1	1	r	r
2	6	6	r	r
3	1	1	r'	r'
4	6	6	r'	r'
5	1	1	g	g
6	6	6	g	g
7	1	1	g'	g'
8	6	6	g'	g'
9	1	1	r	g
10	6	6	r	g
11	1	1	g	r
12	6	6	g	r
13	1	1	r'	g'
14	6	6	r'	g'
15	1	1	g'	r'
16	6	6	g'	r'

one same-shaped pair and one different-shaped pair for each of the 16 possible combinations of size formats and colors.

In stimulus condition 2, members of a stimulus pair were identical in size (size ratio 1), so shape-matching should be relatively easy. For members that differed in color, the discriminability between the colors (two different shades of red or two different shades of green) was low, so color-matching should be relatively difficult. A list of the 16 combinations of size formats and colors that were used in stimulus condition 2 can be obtained from the list in Table 2 by interchanging *g* with *r'* in Combinations 9–16.

In stimulus condition 3, members of a stimulus pair were different in size (size ratio 6), so shape-matching should be relatively difficult (see Larsen et al. 2000, for a recent investigation of the brain mechanisms involved in comparing different-sized stimuli with respect to shape). For members that differed in color, the colors (red versus green) were highly discriminable, so color-matching should be relatively easy. A list of the 16 combinations of size formats and colors that were used in stimulus condition 3 can be obtained from the list in Table 2 by replacing size format combinations *1:1* and *6:6* by size format combinations *1:6* and *6:1*, respectively.

In stimulus condition 4, members of a stimulus pair were different in size (size ratio 6), so shape-matching should be relatively difficult. For members that differed in color, the discriminability between the colors (two different shades of red or two different shades of green) was low, so color-matching should also be relatively difficult. A list of the 16 combinations of size formats and colors that were used in stimulus condition 4 can be obtained from the list in Table 2 by (1) interchanging *g* with *r'* in Combinations 9–16, and (2) replacing size format combinations *1:1* and *6:6* by size format combinations *1:6* and *6:1*, respectively.

Groups

The subjects were assigned to one of two groups. Subjects 1–8 (fixation group) were instructed to maintain fixation at the fixation mark during the PET scans. The importance of maintaining fixation was emphasized at the start of each session. During training, the experimenter monitored fixation by watching the participants' eyes. All of the eight subjects appeared to comply with the instructions. Subjects 9–16 (free-viewing group) received no instructions concerning fixation. In all other respects, treatments of subjects in the two groups were the same.

Design

In each of the two groups, each subject served in two experimental sessions that were separated by 1–5 weeks. Each session comprised eight PET scans, one for each of the factorial combinations of the four stimulus conditions and the two tasks (shape-matching versus color-matching). The complete design is shown in Table 3. Novel random shapes were generated and orderings of stimuli were randomized anew for each scan and each subject.

PET procedure

PET scans were obtained using an 18-ring GE-Advance scanner (General Electric Medical Systems, Milwaukee, Wis., USA) operating in 3-D acquisition mode, producing 35 image slices with an interslice distance of 4.25 mm. The total axial field of view was 15.2 cm with an approximate in-plane resolution of 5 mm. The technical specifications have been described elsewhere (DeGrado et al. 1994). Head movements were limited by head-holders constructed of moulded foam.

For each scan the subject received a bolus injection of 200 MBq (5.7 mCi) $H_2^{15}O$. The isotope was administered manually via an antecubital intravenous catheter over 3–5 s. The experimental task (shape-matching or color-matching) was initiated approximately 45 s prior to isotope arrival to the brain, continued during the 90-s acquisition period, and further continued for about 1 min, until the three blocks of 32 stimulus pairs had been presented. The interscan interval was 10 min.

Before the activation sessions, a 10-min transmission scan was performed for attenuation correction. Images were reconstructed with a 4.0-mm Hanning filter transaxially and an 8.5-mm Ramp filter axially. The resulting distribution images of time-integrated counts were used as indirect measurements of the regional neural activity.

Table 3 Design. Stimulus conditions 1–4 are defined in Table 1. For $i=1,..., 4$, s_i stimulus condition i with shape-matching instructions; c_i stimulus condition i with color-matching instructions. Subjects 1–8 formed the fixation group; subjects 9–16 formed the free-viewing group

Subjects	Session 1 Scan				Session 2 Scan			
	1 2	3 4	5 6	7 8	1 2	3 4	5 6	7 8
1, 9	s_1 c_1	s_2 c_2	s_3 c_3	s_4 c_4	c_4 s_4	c_3 s_3	c_2 s_2	c_1 s_1
2, 10	s_2 c_2	s_3 c_3	s_4 c_4	s_1 c_1	c_1 s_1	c_4 s_4	c_3 s_3	c_2 s_2
3, 11	s_3 c_3	s_4 c_4	s_1 c_1	s_2 c_2	c_2 s_2	c_1 s_1	c_4 s_4	c_3 s_3
4, 12	s_4 c_4	s_1 c_1	s_2 c_2	s_3 c_3	c_3 s_3	c_2 s_2	c_1 s_1	c_4 s_4
5, 13	c_1 s_1	c_2 s_2	c_3 s_3	c_4 s_4	s_4 c_4	s_3 c_3	s_2 c_2	s_1 c_1
6, 14	c_2 s_2	c_3 s_3	c_4 s_4	c_1 s_1	s_1 c_1	s_4 c_4	s_3 c_3	s_2 c_2
7, 15	c_3 s_3	c_4 s_4	c_1 s_1	c_2 s_2	s_2 c_2	s_1 c_1	s_4 c_4	s_3 c_3
8, 16	c_4 s_4	c_1 s_1	c_2 s_2	c_3 s_3	s_3 c_3	s_2 c_2	s_1 c_1	s_4 c_4

Table 4 Reaction times and error rates. *SE* standard error of mean reaction time

Stimuli			Shape judgments			Color judgments		
Type of pair	Size ratio	Color discrim-inability	Reaction time (ms)	SE	Error rate (%)	Reaction time (ms)	SE	Error rate (%)
Fixation group								
Same	1	High	880	38	11.0	633	23	2.9
		Low	874	48	8.9	686	25	2.9
	6	High	907	39	16.8	659	29	3.2
		Low	914	35	15.2	690	18	5.2
Different	1	High	915	32	15.5	646	25	1.4
		Low	917	47	16.5	718	20	2.8
	6	High	946	34	20.8	675	35	1.8
		Low	951	36	21.2	722	17	3.6
Free-viewing group								
Same	1	High	914	40	6.4	704	43	2.1
		Low	904	37	3.8	866	44	7.4
	6	High	967	39	8.6	746	53	4.6
		Low	966	38	10.5	874	48	10.6
Different	1	High	950	40	7.8	690	36	1.9
		Low	941	39	7.4	873	45	11.4
	6	High	972	43	12.8	727	55	2.4
		Low	983	49	15.6	903	49	11.1

Magnetic resonance image (MRI) scanning

For accurate anatomical localization of activated foci, structural MRI scanning was performed on the eight subjects in the fixation group. Scans were performed with a 1.5-T Vision scanner (Siemens, Erlangen, Germany) using a 3-D magnetization-prepared rapid-acquisition gradient-echo (MPRAGE) sequence (repetition time 11 ms, echo time 4 ms, inversion time 100 ms, flip angle 15°). The images were acquired in the sagittal plane with an in-plane resolution of 0.98 mm and a slice thickness of 1.0 mm. The number of planes was 170 and the in-plane matrix dimensions were 256×256.

Image analysis

For all subjects the complete brain volume was sampled. Image analysis was performed using Statistical Parametric Mapping software (SPM96; Wellcome Department of Cognitive Neurology, London, UK; Frackowiak and Friston 1994). All intra-subject images were aligned on a voxel-by-voxel basis using a 3-D automated 6-parameter rigid body transformation (AIR 3.0; Woods et al. 1992), and the anatomical MRI scans were co-registered to the individual averages of the 16 aligned PET scans. The average PET scans and corresponding anatomical MRI scans were subsequently transformed into the standard stereotactic atlas of Talairach and Tournoux (1988) using the PET template defined by the Montreal Neurological Institute (MNI; Friston et al. 1995a). The stereotactically normalized images consisted of 68 planes of 2×2×2 mm voxels. Before statistical analysis, images were filtered by a 16-mm (FWHM) isotropic Gaussian filter to increase the signal-to-noise ratio and to accommodate residual variability in morphological and topographical anatomy that was not accounted for by the stereotactic normalization process (Friston 1994). Differences in global activity were removed by proportional normalization to a value of 50. Only intracerebral areas that did not change significantly ($P>0.05$) between conditions were selected to represent global activity following the iterative approach described by Andersson (1997). The null hypothesis of no regionally specific activation effects of the experimental conditions was tested by comparing conditions on a voxel-by-voxel basis. The resulting set of voxel values constituted a statistical parametric map of the *t*-statistic, SPM{*t*}. A transformation of values from the SPM{*t*} into the unit Gaussian distribution using a probability integral transform allowed changes to be reported in Z-scores (SPM{Z}). Unless otherwise indicated, voxels were considered significant if their Z-score exceeded a threshold of $P<0.05$ after correction for multiple comparisons. This threshold was estimated according to Friston et al. (1995b) using the theory of Gaussian fields.

Results and discussion

Behavioral data

Table 4 shows group mean reaction time for correct responses and mean rate of errors as functions of task (shape- versus color-matching), size ratio within stimulus pairs (1 versus 6), color discriminability within stimulus pairs (high versus low), type of pair ("same" versus "different"), and group (fixation versus free-viewing). The two dependent variables (reaction time and error rate) were highly correlated. In the fixation group, the Pearson product-moment correlation coefficient between the mean reaction time and the mean rate of errors across the 16 possible combinations of task, size ratio, color discriminability, and type of pair was 0.95. In the free-viewing group, the corresponding correlation was 0.78.

The reaction times were subjected to a repeated-measures analysis of variance with group as a between-subjects variable. The main effect of task was highly significant, $F_{(1,14)}=286.96$, $P<0.0001$; the mean reaction time for shape-matching exceeded the mean reaction time for color-matching by 193 ms. Main effects of size ratio, color discriminability, and type of pair were also significant. Mean reaction time for pairs with a size ratio 6 exceeded mean reaction time for pairs with a size ratio 1 by 31 ms, $F_{(1,14)}=12.87$, $P<0.01$; mean reaction time for

Shape - color Color - shape Difficult color - easy color

A) B) C)

SPM{Z}, p < 0.05, corrected
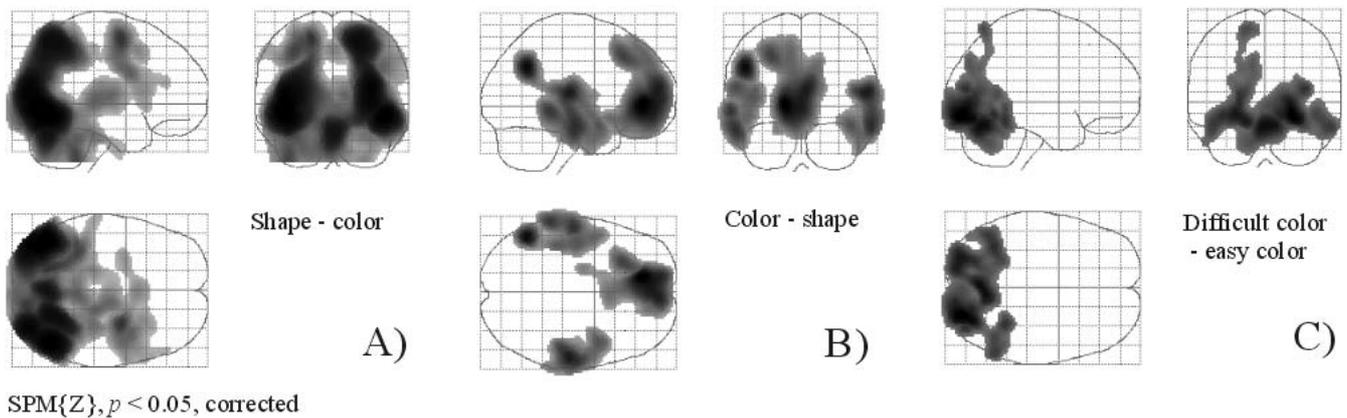
Fig. 2A–C Maximum intensity statistical parametric map projections of significant clusters of voxels (*P*<0.05, corrected for multiple comparisons; SPM{Z} >2.33). **A** The shape-color contrast (the shape-matching minus color-matching difference image, at locations where the mean regional cerebral blood flow across subjects and conditions was higher for shape-matching than for color-matching). **B** The reverse (color-minus-shape) contrast. **C** The difficult-minus-easy color-matching contrast

pairs with low color discriminability exceeded mean reaction time for pairs with high color discriminability by 53 ms, $F_{(1,14)}$=82.31, *P*<0.0001; mean reaction time for "different" pairs exceeded mean reaction time for "same" pairs by 22 ms, $F_{(1,14)}$=16.74, *P*<0.001. The main effect of group was not significant, $F_{(1,14)}$=2.36, *P*>0.10.

The effect of task was significantly greater in the fixation group than in the free-viewing group, $F_{(1, 14)}$=13.06, *P*<0.01. In the fixation group, the mean reaction time for shape-matching exceeded the mean reaction time for color-matching by 234 ms; in the free-viewing group, the corresponding difference was 152 ms.

Color discriminability showed significant interactions with task, type of pair, group, and the combination of group and task. As expected, the effect of color discriminability was much greater in color-matching (where the effect was 107 ms) than in shape-matching (where the effect was 0 ms), $F_{(1,14)}$=89.17, *P*<0.0001. The effect of color discriminability was also greater for "different" than for "same" pairs [$F_{(1,14)}$=14.93, *P*<0.001] and greater in the free-viewing than in the fixation group [$F_{(1,14)}$=21.09, *P*<0.001]. The greater strength of the effect of color discriminability in the free-viewing group was found in color-matching, but not in shape-matching (where neither group showed any effect of color discriminability); this was evidenced by the three-way interaction between color discriminability, group, and task, $F_{(1,14)}$=25.97, *P*<0.001. No other interaction effects were reliable, not even the two-way interaction between size ratio and task, $F_{(1,14)}$=2.51, *P*>0.10.

PET data

The PET data showed nearly the same effects of the within-subject variables (task, size ratio, and color discriminability) on rCBF in the two experimental groups (fixation versus free-viewing). For each within-subject variable, we contrasted the effect of the variable in the fixation group against the effect of the variable in the free-viewing group. The only significant difference between the groups with respect to the effects of the within-subject variables was found in the right frontal operculum, where a cluster of voxels with focus at location 30, 24, 0 (Talairach coordinates; Talairach and Tournoux 1988) showed greater effect of task (by the color-minus-shape contrast) in the free-viewing than in the fixation group, SPM{Z} =4.58, *P*<0.05.

Task

Maximum intensity SPM projections of clusters of voxels that showed significantly greater rCBF in shape-matching than in color-matching (i.e., significant activation by the shape minus color contrast) are displayed in Fig. 2A. Similar projections of clusters of voxels that showed significantly greater rCBF in color- than in shape-matching (i.e., significant activation by the color minus shape contrast) are displayed in Fig. 2B. Transverse sections of the 3-D SPM images are shown in Fig. 3, and the anatomical locations of voxels with maximum Z-scores (one for each significant activation cluster) are listed in Table 5. The data are averaged across all subjects and experimental conditions. Neither the shape-color nor the color-shape contrast showed any significant interactions with size ratio or color discriminability.

Shape-color contrast

As noted above, mean reaction time for shape-matching exceeded mean reaction time for color-matching by nearly 200 ms. By the shape-color contrast shown in Table 5 and Figs. 2 and 3, the rCBF generated by shape-matching was also significantly greater than the rCBF generated by color-matching throughout most of the occipital cortex, a large part of the parietal cortex (with
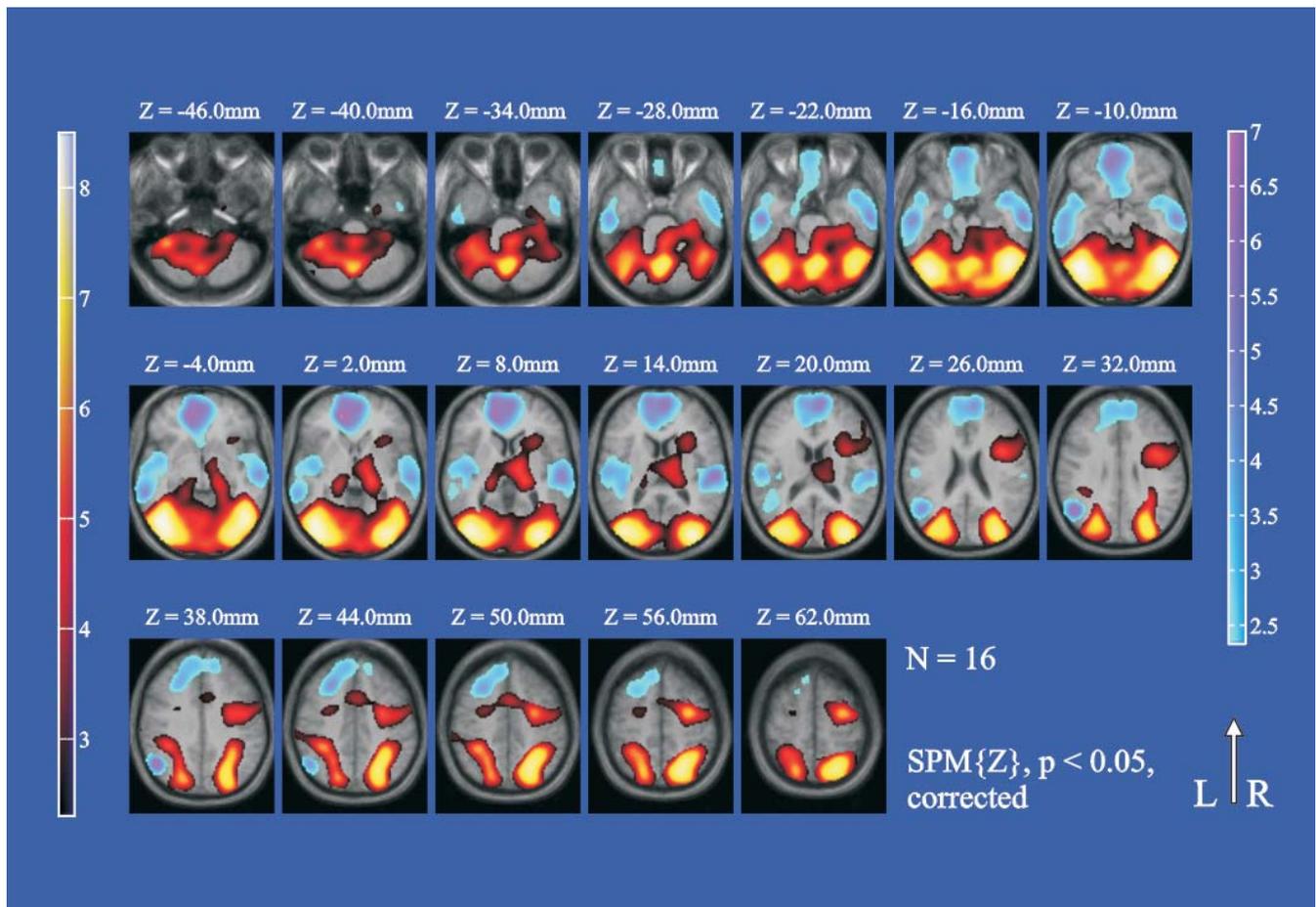
Fig. 3 Transverse sections of the statistical parametric map of shape-color and color-shape contrasts. Z-scores for the shape-color contrast are shown on a hot metal color scale (*left*); Z-scores for the reverse contrast are shown on a cool (cyan-blue-violet) scale (*right*). The contrasts are rendered on the average image of the normalized magnetic resonance brain images of the eight MRI-scanned subjects. Distances above/below the anterior commissure-posterior commissure (AC-PC) plane are given in millimeters. For all clusters of voxels $P<0.05$, corrected for multiple comparisons

bilateral foci in the posterior superior parietal lobule), and a smaller region in the frontal cortex. Subcortical activations were observed in the thalamus and the cerebellum.

None of the ten foci of significant activation listed in Table 5 showed less activation in the fixation than in the free-viewing group. To further evaluate the role of eye movements, we tested for interaction between shape-color contrast and experimental group (fixation versus free-viewing) in a region of interest consisting of the set of voxels in which the shape-color contrast was significant at a level of $P=0.001$ (uncorrected). No significant interaction was found, $P>0.05$.

Structural MRIs were obtained for the eight subjects in the fixation group, which made it possible to localize the activations in the occipital cortex for each of these subjects with fairly high precision. We were particularly concerned with testing for attentional effects in the calcarine sulcus, where primary visual cortex is found. One subject showed no activation in the calcarine or in the vicinity of the calcarine sulcus. Each of the other

seven subjects showed activation in the calcarine sulcus. For the seven subjects, activations in the calcarine sulcus were significant at P-levels of 0.01, 0.00005, 0.06, 0.5, 0.02, 0.06, and 0.00005, respectively. For the group of eight subjects as a whole, the increase in rCBF in the calcarine sulcus was highly significant, $\chi^2_{(16)}>69.29$, $P<0.0001$ (cf., p 49 in Winer 1971).

We compared our PET findings with the fMRI data collected by Martínez and colleagues (Table 1 in Martínez et al. 1999) in their study of spatial selection of targets in the left versus the right visual field. At the locations given as Talairach coordinates in Table 6, Martínez et al. found foci of fMRI activation clusters produced by attentional selection of stimuli in the contralateral visual field. As indicated in Table 6, the locations seemed to be in functional visual areas V1, V2, V3, VP, V3A, and V4v, in other regions of the posterior fusiform and the middle occipital gyri, and in the posterior parietal lobe. Table 6 shows the Z-scores and the associated, uncorrected levels of significance for voxels at the same locations by the shape-color contrast in

Table 5 Shape-matching versus color-matching: foci of activation. For each significant (P<0.05) activation cluster, the anatomical location of the voxel with the maximum Z-score is given in Talairach coordinates. The level of significance (α) of the Z-score is corrected for multiple comparisons. Three other, nonsignificant (ns) foci have been included

Contrast	Anatomical localization	Coordinates			Z-score	Significance α
		x	y	z		
Shape-color	L inferior/middle occipital gyrus	−42	−70	−8	8.10	0.0001
	R inferior/middle occipital gyrus	46	−66	−10	7.78	0.0001
	R middle occipital gyrus	36	−86	14	7.72	0.0001
	R posterior superior parietal lobule	22	−66	56	7.54	0.0001
	L posterior superior parietal lobule	−18	−70	58	6.30	0.0001
	Cerebellar vermis	−2	−72	−24	7.32	0.0001
	L cerebellum	−20	−68	−50	4.50	0.05
	R posterior superior frontal sulcus	30	−4	58	6.11	0.0001
	R middle frontal gyrus/precentral sulcus	42	2	32	4.48	0.05
	L middle frontal gyrus/precentral sulcus	−46	0	32	3.34	ns
	L posterior superior frontal sulcus	−28	−2	48	3.34	ns
	R posterior thalamus	18	−26	4	5.17	0.005
	L posterior thalamus	−18	−30	4	4.07	ns
Color-shape	L/R anterior cingulate gyri	−14	44	2	6.57	0.0001
	L/R superior frontal gyri	4	56	14	5.72	0.0001
	L anterior middle frontal gyrus	−26	28	44	4.85	0.01
	L angular/supramarginal/superior temporal gyrus	−48	−58	34	6.16	0.0001
	R superior temporal gyrus	58	−22	12	5.76	0.0001
	L superior temporal gyrus	−56	−18	18	4.48	0.05
	R middle temporal gyrus	62	−16	−16	5.27	0.001
	L middle temporal gyrus	−58	−18	−20	5.14	0.005

the present study. At each of the 21 locations, the rCBF in the shape-matching task was significantly higher than that in the color-matching task.

We also compared our findings with those of Brefczynski and DeYoe (1999). The shape-color contrast in our study showed activation everywhere in the region in which Brefczynski and DeYoe found attention-driven activity. In the anterior-posterior extremes of the supposed V1/V2 region, indexed by mean Talairach coordinates −15, −75, 10, and −20, −97, −4, the Z-scores in our data were 4.97 and 5.64, respectively. In the anterior-posterior extremes of the region of attentional modulation in the ventral occipito-temporal cortex, indexed by mean coordinates −20, −63, −8 and −25, −89, −17, the Z-scores in our data were 4.79 and 5.97; for each of the four Z-scores, P<0.001 (uncorrected).

Brefczynski and DeYoe noted that they "did not examine the lateral geniculate nucleus" (see p 373 in Brefczynski and DeYoe 1999). The thalamic activations found by the shape-color contrast in our whole-brain PET study peaked right in the middle of a small posterior thalamic region comprising the lateral geniculate nucleus (LGN), the pulvinar, and adjacent parts of the reticular nucleus. Each of the LGN, the pulvinar, and the reticular nucleus are involved in visual processing. The LGN is the main relay station for visual signals on the route from retinal ganglion cells to area V1, and V1 feeds massively back to the LGN (cf. Casagrande and Norton 1991; Garey et al. 1991; see also Mumford 1991). The reticular thalamic nucleus is interconnected with LGN in a loop that may cause inhibition in LGN relay cells (Garey et al. 1991; see also Crick 1984), and the pulvinar is interconnected with numerous visual cortical areas including V1 (Chalupa 1991; see also LaBerge 1990, 1995; LaBerge and Buchsbaum 1990).

The shape-color contrast showed activation in a prefrontal cortical region that seems implicated in visual short-term memory (working memory). We found a highly significant focus in the right posterior superior frontal sulcus (see Table 5). The focus (Talairach coordinates 30, −4, 58) was fairly close to the focus of activation reported by Courtney et al. (1998) for a region in the right prefrontal cortex specialized for spatial working memory (mean Talairach coordinates 27, −5, 49; SD at 5). There was a corresponding (but nonsignificant) focus in the left hemisphere (Talairach coordinates −28, −2, 48), close to the focus of activation reported by Courtney et al. (1998) for a region in the left prefrontal cortex specialized for spatial working memory (mean Talairach coordinates −31, −7, 46). We also found nearly symmetric foci of activation on the borderline between the middle frontal gyri and the precentral sulci. Corrected for multiple comparisons, the right-hemisphere focus was significant, but the left-hemisphere focus was not (cf. Table 5). The activations in the middle frontal gyri appear to lie in regions that show sustained activity during delays in visual working memory tasks without being specialized for retention of spatial information (cf., Fig. 2 and Note 24 in Courtney et al. 1998).

The significant activations in the cerebellum were not anticipated. They add to the growing evidence that the cerebellum contributes not only to motor control but also to perceptual and cognitive processing (see, e.g., Allen et al. 1997; Gao et al. 1996; Larsen et al. 2000; Leiner et al. 1995; Luft et al. 1998; Nobre et al. 1997).

Table 6 Effects at locations activated by spatial attention in study by Martínez et al. (1999). At the indicated locations (given in Talairach coordinates), Martínez et al. (1999) reported significant correlations between neural activity (measured by functional magnetic resonance imaging, fMRI) and direction of attention (left versus right visual field). At these same locations, we have indicated Z-scores and associated levels of significance (α) found by the shape-color contrast in the present study (*V1, V2, V3, VP, V3A,* and *V4v* are functional visual areas; *Fusi.* posterior fusiform gyrus; *Mid.occ.* middle occipital gyrus; *Post.par.* posterior parietal lobe)

Ventral		V1	V2	VP	>V4v	Fusi.	
Left	Location	–9, –90, –5	–12, –79, –8	–16, –75, –7	–26, –76, –11	–31, –60, –11	
	Z-score	5.10	5.11	5.40	7.45	6.28	
	α	10^{-6}	10^{-6}	10^{-7}	10^{-13}	10^{-9}	
Right	Location	7, –88, 0	7, –78, –3	9, –74, –8	19, –70, 11	33, –61, –13	
	Z-score	4.20	3.94	4.69	4.78	7.20	
	α	10^{-4}	10^{-4}	10^{-5}	10^{-6}	10^{-12}	
Dorsal		V1	V2	V3	V3A	Mid. occ.	Post. par.
Left	Location	–8, –91, 0	–10, –85, 0	–22, –85, 14	–	–29, –75, 19	–29, –55, 50
	Z-score	5.22	5.43	7.42	–	7.42	5.06
	α	10^{-7}	10^{-7}	10^{-13}	–	10^{-13}	10^{-6}
Right	Location	7, –89, 1	7, –84, 5	21, –88, 13	24, –81, 19	27, –75, 13	28, –49, 57
	Z-score	4.16	3.42	6.86	7.34	7.25	6.93
	α	10^{-4}	10^{-3}	10^{-11}	10^{-12}	10^{-12}	10^{-11}

Color-shape contrast

The results of the reverse analysis, color-shape contrast, are also indicated in Table 5 and Figs. 2 and 3. As can be seen, the color-shape contrast showed bilateral increases in rCBF in the anterior cingulate gyri, superior frontal gyri, and superior and middle temporal gyri. The color-shape contrast also showed unilateral increases in rCBF in two regions in the left hemisphere: one in the anterior middle frontal gyrus, and one at the junction of the angular, the supramarginal, and the superior temporal gyri. The pattern of activations (in particular, the activations in the anterior cingulate and in the temporal cortex) shows similarities to activation patterns observed in the Stroop color-word interference task (see Carter et al. 1995; George et al. 1994; Pardo et al. 1990; Taylor et al. 1994). It is possible that the activations reflect cognitive operations that inhibit decision procedures based on shape information in favor of procedures based on color information.

To evaluate the role of eye movements, we tested for interaction between color-shape contrast and experimental group (fixation versus free-viewing) in a region of interest consisting of the set of voxels in which the color-shape contrast was significant at a probability level of 0.001 (uncorrected). No significant interaction was found, $P>0.05$. Actually no voxel in which the color-shape contrast was significant at a probability level of 0.05 (uncorrected) showed an uncorrected P-value below 0.05 for the interaction.

Size ratio

Corrected for multiple comparisons, the PET data showed no significant main effects of size ratio, no significant interactions of size ratio with task, and no significant simple effects of size ratio for either shape- or color-matching. The behavioral data for shape-matching showed a clear decrement in performance when the stimulus patterns to be compared were different in size (size ratio 6 versus size ratio 1), but the decrement appeared as a substantial increase in the rate of errors (from 9.7% to 15.2%) and only a minor increase in mean reaction time (from 912 ms to 951 ms) (for related behavioral data, see Larsen et al. 1999). In a related one-back match-to-sample PET study in which an alternating-size condition was contrasted with fixed-size conditions, Larsen et al. (2000) found both a greater effect of size ratio in mean reaction time and significant activations in the posterior parietal cortex (bilaterally, in the subparietal sulci), the occipital-temporal-parietal transition zone (predominantly in the left hemisphere), area MT (left), and vermis (bilaterally). Although the temporal effects of size ratio were small in the present study, the voxels in which Larsen et al. (2000, see Table 2 of that report) found foci of significant activation also showed activation in the present study, and in each of these voxels, the activation approached significance; with Z-scores ranging between 1.28 and 1.38, $0.05< P<0.10$ (uncorrected).

Color discriminability

Like the reaction time data, the PET data (corrected for multiple comparisons) showed both significant main effects of color discriminability and significant interactions of color discriminability with task. Owing to the significant interactions, our major analyses concerned the simple effects of color discriminability in each of the two tasks. Corrected for multiple comparisons, there were no significant effects of color discriminability in the shape-
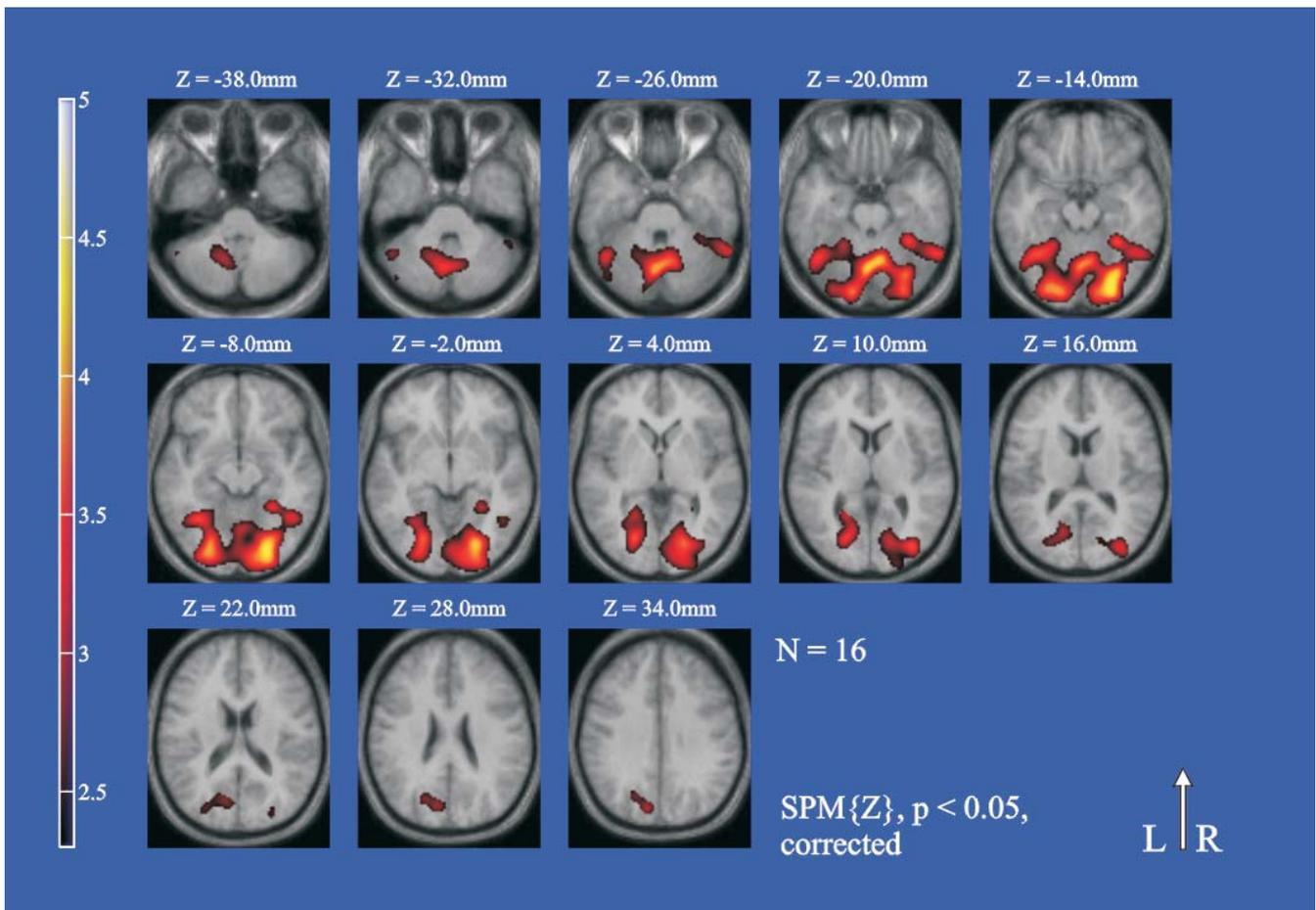
Fig. 4 Transverse sections of the statistical parametric map of the color discriminability contrast (difficult minus easy color-matching). Z-scores are mapped to a hot metal color scale (*left*). The contrast is rendered on the average image of the normalized magnetic resonance brain images of the eight MRI-scanned subjects. Distances above/below the AC-PC plane are given in millimeters. For all clusters of voxels $P<0.05$, corrected for multiple comparisons

Table 7 Difficult versus easy color discrimination: foci of activation. One activation cluster, which included a large part of the occipital cortex, was significant at a level of 0.05. For this cluster, the anatomical location of the voxel with the maximum Z-score is given in Talairach coordinates. The level of significance (α) is corrected for multiple comparisons. Two nonsignificant (*ns*) foci are also listed

Anatomical localization	Coordinates			Z-score	Significance
	x	y	z		α
R posterior fusiform gyrus	26	–86	–12	4.49	0.03
L posterior fusiform gyrus	–26	–86	–12	3.98	ns
Cerebellar vermis	0	–68	–20	4.17	ns

matching task, but extensive effects in the color-matching task. The behavioral data for color-matching showed a substantial (107 ms) increment in mean reaction time when color discriminability was low. As indicated in Table 7 and Figs. 2 and 4, the corresponding PET contrast (difficult minus easy color discrimination) showed significant activation in a large part of the occipital cortex. The reverse contrast (easy minus difficult color discrimination) showed no significant activation.

The occipital activation found by the contrast between difficult and easy color discrimination had bilaterally symmetrical foci (Talairach coordinates ±26, –86, –12) in the posterior fusiform gyri near the supposed location of human V4 (cf. McKeefry and Zeki 1997; Sakai et al. 1995; Zeki et al. 1991). Considering that mean reaction time was delayed by about 100 ms for difficult color discrimination, compared with easy, it seems likely that the increase in rCBF in the fusiform gyri was due to increase in the duration of processing color information in V4. Other studies have yielded results that support this interpretation. In subjects asked to compare the colors of two successively displayed stimuli (Clark et al. 1997;

Corbetta et al. 1990) or detect the faint dimming of one stimulus in a stream of otherwise identically colored stimuli (Annlo-Vento et al. 1998), both prominent ERP components and hemodynamic responses measured by PET and fMRI have been referred to V4 (see also Nobre et al. 1998). The indicated location of V4 in Talairach space has varied a little between studies; a typical set of Talairach coordinates is (±28, –79, –16) (cf., Table 2 in McKeefry and Zeki 1997).

We tested the activation in the two prefrontal voxels in which the shape-color contrast had shown significant foci of activation. In the focus on the borderline between the right middle frontal gyrus and the precentral sulcus (Talairach coordinates 42, 2, 32), the difficult-minus-easy color discrimination contrast yielded a Z-score of 1.86, $P<0.05$ (uncorrected). In the focus in the right posterior superior frontal sulcus (Talairach coordinates 30, –4, 58), it yielded $Z=1.25$, $P=0.11$ (uncorrected).

Concluding discussion

The main results of the reported PET study were found by contrasting the distribution of rCBF during performance of the shape-matching task with that during the much less demanding color-matching task. The contrast showed widespread attentional effects (effects of the experimental task) in the visual system, including effects in the primary visual (striate) cortex and effects in the thalamus with focus in a region comprising the LGN, the pulvinar, and adjacent parts of the reticular nucleus. The contrast also showed activation in a prefrontal cortical region (posterior parts of the superior frontal sulcus and the middle frontal gyrus) that seems implicated in visual short-term (working) memory (VSTM). The prefrontal activation presumably reflects that the stimuli were retained in VSTM for a longer period of time in the shape-matching than in the color-matching task. We conjecture that the attentional effects in the thalamus and the striate cortex were generated by feedback signals from the prefrontal cortex via the posterior parietal cortex and extrastriate visual areas to striate cortex and the thalamus (cf. Büchel et al. 1998; Selemon and Goldman-Rakic 1988). The feedback loop between early visual areas and the prefrontal cortex should serve to maintain visual representations of attentionally selected stimuli in active memory (VSTM) until the processing of the stimuli is completed.

Many other possible explanations of the pattern of activations found by the shape-color contrast may be considered. Firstly, instead of assuming that the stimuli were retained in VSTM for a longer period in the shape-matching than in the color-matching task, the greater activation levels in the shape task might be explained by assuming that more information must be kept active in order to compare the shape of one polygon with another than is required to compare the color of one polygon with another. To keep more information active in the shape task, the number of activated cells or the magnitude of activation of individual cells may have been increased rather than the duration of the activation being increased. However, the fact that reaction times were much longer in the shape task supports our hypothesis that the duration of activation was longer in the shape task.

Secondly, instead of, or in addition to, the hypothesized difference in VSTM retention, there may have been (1) more nonspecific alerting or arousal in the shape task, (2) more sustained and intensive deployment of spatial attention in the shape task, or (3) more extensive attentional scanning and switching in the shape task. Thus, the prefrontal activation may have been attentional without being related to activity in short-term memory (cf. Corbetta and Shulman 1998; also see Awh et al. 1999; Coull et al. 2000; LaBar et al. 1999). Still, the results of Courtney et al. (1998) support the hypothesis that the activations we found in the posterior parts of the superior frontal sulcus and the middle frontal gyrus included VSTM activity.

Finally, in the suggested interpretation of the pattern of activations found by the shape-color contrast, the increased prefrontal activation was functionally responsible for the increased activation in posterior visual processing areas. It is possible that the prefrontal and posterior visual activations were correlated without being causally related. In particular, instead of being caused by feedback from prefrontal cortex, it is possible that the striate and thalamic activations were caused by feedforward mechanisms. However, the hypothesis that attentional effects in the striate cortex and the thalamus are due to feedback seems preferable. The hypothesis seems consistent with all available evidence (including the evidence by Luck et al. 1997 against the notion of sustained top-down activation of neurons in V1 during spatial attention), and it explains why studies using PET and fMRI have shown attentional effects in the striate cortex (Brefczynski and DeYoe 1999; Martínez et al. 1999; this article) and the thalamus (LaBerge and Buchsbaum 1990; this article), whereas studies of early ERP components (e.g., Clark and Hillyard 1996) have supported the assumption that the initial sensory response of the striate cortex is unaffected by attention.

References

Allen G, Buxton RB, Wong EC, Courchesne E (1997) Attentional activation of the cerebellum independent of motor involvement. Science 275:1940–1943

Andersson JL (1997) How to estimate global activity independent of changes in local activity. Neuroimage 6:237–244

Annlo-Vento L, Luck SJ, Hillyard SA (1998) Spatio-temporal dynamics of attention to color: evidence from human electrophysiology. Hum Brain Mapp 6:216–238

Awh E, Jonides J, Smith EE, Buxton RB, Frank LR, Love T, Wong EC, Gmeindl L (1999) Rehearsal in spatial working memory: evidence from neuroimaging. Psychol Sci 10:433–437

Brefczynski JA, DeYoe EA (1999) A physiological correlate of the "spotlight" of visual attention. Nat Neurosci 2:370–374

Büchel C, Josephs O, Rees G, Turner R, Frith CD, Friston KJ (1998) The functional anatomy of attention to visual motion: a functional MRI study. Brain 121:1281–1294

Bundesen C (1990) A theory of visual attention. Psychol Rev 97:523–547

Bundesen C (1991) Towards a neural network implementation of TVA. Paper presented at the First Meeting of the HFSP Research Group on Brain Mechanisms of Visual Selection, School of Psychology, University of Birmingham, UK

Bundesen C (1998) A computational theory of visual attention. Phil Trans R Soc Lond B 353:1271–1281

Bundesen C (2002) A general theory of visual attention. In: Bäckman L, von Hofsten C (eds) Psychology at the turn of the millennium, vol 1. Cognitive, biological, and health perspectives. Psychology Press, Hove UK

Bundesen C, Larsen A (1975) Visual transformation of size. J Exp Psychol Hum Percept Perform 1:214–220

Carter CS, Mintun M, Cohen JD (1995) Interference and facilitation effects during selective attention: an $H_2^{15}O$ PET study of Stroop task performance. Neuroimage 2:264–272

Casagrande VA, Norton TT (1991) Lateral geniculate nucleus: a review of its physiology and function. In: Leventhal AG (ed) The neural basis of visual function. Macmillan, London, pp 41–84

Chalupa LM (1991) Visual function of the pulvinar. In: Leventhal AG (ed) The neural basis of visual function. Macmillan, London, pp 140–159

Clark VP, Hillyard SA (1996) Spatial selective attention affects early extrastriate but not striate components of the visual evoked potential. J Cogn Neurosci 8:387–402

Clark VP, Fan S, Hillyard SA (1995) Identification of early visually evoked potential generators by retinotopic and topographic analyses. Hum Brain Mapp 2:170–187

Clark VP, Parasuraman R, Keil K, Kulansky R, Fannon S, Maisog JM, Ungerleider LG, Haxby JV (1997) Selective attention to face identity and color studied with fMRI. Hum Brain Mapp 5:293–297

Corbetta M, Shulman GL (1998) Human cortical mechanisms of visual attention during orienting and search. Phil Trans R Soc Lond B 353:1353–1362

Corbetta M, Miezin FM, Dobmeyer S, Shulman GL, Petersen SE (1990) Attentional modulation of neural processing of shape, color, and velocity in humans. Science 248:1556–1559

Coull JT, Frith CD, Büchel C, Nobre AC (2000) Orienting attention in time: behavioural and neuroanatomical distinction between exogenous and endogenous shifts. Neuropsychologia 38:808–819

Courtney SM, Petit L, Maisog JM, Ungerleider LG, Haxby JV (1998) An area specialized for spatial working memory in human frontal cortex. Science 279:1347–1351

Crick F (1984) Function of the thalamic reticular complex: the searchlight hypothesis. Proc Natl Acad Sci USA 81:4586–4590

DeGrado TR, Turkington TG, Williams JJ, Stearns CW, Hoffman JM, Coleman RE (1994) Performance characteristics of a whole-body PET scanner. J Nucl Med 35:1398–1406

Duncan J, Bundesen C, Olson A, Humphreys G, Chavda S, Shibuya H (1999) Systematic analysis of deficits in visual attention. J Exp Psychol Gen 128:450–478

Frackowiak RSJ, Friston KJ (1994) Functional neuroanatomy of the human brain: positron emission tomography: a new neuroanatomical technique. J Anatomy 184:211–225

Friston KJ (1994) Statistical parametric mapping. In: Thatcher R, Hallet M, Zeffiro T, Roy JE, Huerta M (eds) Functional neuroimaging: technical foundations. Academic Press, San Diego, pp 79–94

Friston KJ, Ashburner J, Frith CD, Poline J, Heather JD, Frackowiak RSJ (1995a) Spatial registration and normalization of images. Hum Brain Mapp 2:165–189

Friston KJ, Holmes AP, Worsley KJ, Poline J, Frith CD, Frackowiak RSJ (1995b) Statistical parametric maps in functional imaging: a general linear approach. Hum Brain Mapp 2:189–210

Gao J-H, Parsons LM, Bower J, Xiong J, Li J, Fox PT (1996) Cerebellum implicated in sensory acquisition and discrimination rather than motor control. Science 272:545–547

Garey LJ, Dreher B, Robinson SR (1991) The organization of the visual thalamus. In: Dreher B, Robinson SR (eds) Neuroanatomy of the visual pathways and their development. Macmillan, London, pp 176–234

George MS, Ketter TA, Parekh PI, Rosinsky N, Ring H, Casey BJ, Trimble MR, Horwitz B, Herscovitch P, Post RM (1994) Regional brain activity when selecting a response despite interference: an $H_2^{15}O$ PET study of the Stroop and an emotional Stroop. Hum Brain Mapp 1:194–209

Hillyard SA, Hinrichs H, Tempelmann C, Morgan ST, Hansen JC, Scheich H, Heinze H-J (1997) Combining steady-state visual evoked potentials and fMRI to localize brain activity during selective attention. Hum Brain Mapp 5:287–292

Hillyard SA, Vogel EK, Luck SJ (1998) Sensory gain control (amplification) as a mechanism of selective attention: electrophysiological and neuroimaging evidence. Phil Trans R Soc Lond B 353:1257–1270

Kastner S, Pinsk MA, De Weerd P, Desimone R, Ungerleider LG (1999) Increased activity in human visual cortex during directed attention in the absence of visual stimulation. Neuron 22:751–761

LaBar KS, Gitelman DR, Parrish TB, Mesulam M-M (1999) Neuroanatomic overlap of working memory and spatial attention networks: a functional MRI comparison within subjects. Neuroimage 10:695–704

LaBerge D (1990) Thalamic and cortical mechanisms of attention suggested by recent positron emission tomographic experiments. J Cogn Neurosci 2:358–372

LaBerge D (1995) Attentional processing: the brain's art of mindfulness. Harvard University Press, Cambridge, Mass.

LaBerge D, Buchsbaum MS (1990) Positron emission tomographic measurements of pulvinar activity during an attention task. J Neurosci 10:613–619

Larsen A, Bundesen C (1978) Size scaling in visual pattern recognition. J Exp Psychol Hum Percept Perform 4:1–20

Larsen A, McIlhagga W, Bundesen C (1999) Visual pattern matching: effects of size ratio, complexity, and similarity in simultaneous and successive matching. Psychol Res 62:280–288

Larsen A, Bundesen C, Kyllingsbæk S, Paulson OB, Law I (2000) Brain activation during mental transformation of size. J Cogn Neurosci 12:763–774

Leiner HC, Leiner AL, Dow RS (1995) The underestimated cerebellum. Hum Brain Mapp 2:244–254

Logan GD (1996) The CODE theory of visual attention: an integration of space-based and object-based attention. Psychol Rev 103:603–649

Luck SJ, Chelazzi L, Hillyard SA, Desimone R (1997) Neural mechanisms of spatial selective attention in areas V1, V2, and V4 of macaque visual cortex. J Neurophys 77:24–42

Luft AR, Skalej M, Stefanou A, Klose U, Voigt K (1998) Comparing motion- and imagery-related activation in the cerebellum: a functional MRI study. Hum Brain Mapp 6:105–113

Mangun GR, Hopfinger JB, Kussmaul CL, Fletcher EM, Heinze H-J (1997) Covariations in ERP and PET measures of spatial selective attention in human extrastriate visual cortex. Hum Brain Mapp 5:273–279

Martínez A, Anllo-Vento L, Sereno MI, Frank LR, Buxton RB, Dubowitz DJ, Wong EC, Hinrichs H, Heinze H-J, Hillyard SA (1999) Involvement of striate and extrastriate visual cortical areas in spatial attention. Nat Neurosci 2:364–368

McKeefry DJ, Zeki S (1997) The position and topography of the human colour centre as revealed by functional magnetic resonance imaging. Brain 120:2229–2242

Mumford D (1991) On the computational architecture of the neocortex. I. The role of the thalamo-cortical loop. Biol Cybern 65:135–145

Nobre AC, Sebestyen GN, Gitelman DR, Mesulam MM, Frackowiak RSJ, Frith CD (1997) Functional localization of the system for visuospatial attention using positron emission tomography. Brain 120:515–533

Nobre AC, Allison T, McCarthy G (1998) Modulation of human extrastriate visual processing by selective attention to colours and words. Brain 121:1357–1368

Pardo JV, Pardo PJ, Janer KW, Raichle ME (1990) The anterior cingulate cortex mediates processing selection in the Stroop attentional conflict paradigm. Proc Natl Acad Sci USA 87:256–259

Sakai K, Watanabe E, Onodera Y, Uchida I, Kato H, Yamamoto E, Koizumi H, Miyashita Y (1995) Functional mapping of the human colour centre with echo-planar magnetic resonance imaging. Proc R Soc Lond B Biol Sci 261:89–98

Selemon LD, Goldman-Rakic PS (1988) Common cortical and subcortical targets of the dorsolateral prefrontal and posterior parietal cortices in the rhesus monkey: evidence for a distributed neural network subserving spatially guided behavior. J Neurosci 8:4049–4068

Shulman GL, Corbetta M, Buckner RL, Raichle ME, Fiez JA, Miezin FM, Petersen SE (1997) Top-down modulation of early sensory cortex. Cereb Cortex 7:193–206

Smith EE, Jonides J (1997) Working memory: a view from neuroimaging. Cognit Psychol 33:5–42

Talairach J, Tournoux P (1988) Co-planar stereotaxic atlas of the human brain. Thieme Medical Publishers, New York

Taylor SF, Kornblum S, Minoshima S, Oliver LM, Koeppe RA (1994) Changes in medial cortical blood flow with a stimulus-response compatibility task. Neuropsychologia 32:249–255

Winer BJ (1971) Statistical principles in experimental design, 2nd edn. McGraw-Hill, New York

Woldorff MG, Fox PT, Matzke M, Lancaster JL, Veeraswamy S, Zamarripa F, Seabolt M, Glass T, Gao JH, Martin CC, Jerabek P (1997) Retinotopic organization of early visual spatial attention effects as revealed by PET and ERPs. Hum Brain Mapp 5:280–286

Woods RP, Cherry SR, Mazziotta JC (1992) Rapid automated algorithm for aligning and reslicing PET images. J Comput Assist Tomogr 16:620–633

Zeki S, Watson JDG, Lueck CJ, Friston KJ, Kennard C, Frackowiak RSJ (1991) A direct demonstration of functional specialization in human visual cortex. J Neurosci 11:641–649